Received 14 March 2025; revised 16 April 2025; accepted 18 April 2025. Date of publication 21 April 2025;
date of current version 7 May 2025. The review of this article was arranged by Associate Editor Yongchang Zhang.

*Digital Object Identifier 10.1109/OJPEL.2025.3563134*

# Sequential Model Predictive Torque Control for Six-Phase Machines Without Weighting Factors

**JORGE RODAS [1] (Senior Member, IEEE), OSVALDO GONZALEZ [1], PAOLA MAIDANA [1], CHRISTIAN MEDINA [1], JESÚS DOVAL-GANDOY [2] (Member, IEEE), MARGARITA NORAMBUENA [3] (Senior Member, IEEE), MAGNO AYALA [1] (Member, IEEE), AND JOSE RODRIGUEZ [4] (Life Fellow, IEEE)**

[1]Department of Electronics and Mechatronics Engineering, Facultad de Ingeniería Universidad Nacional de Asunción, Luque 110948, Paraguay
[2]Applied Power Electronics Technology Research Group, CINTECX, Universidad de Vigo, 36310 Vigo, Spain
[3]Department of Electrical Engineering, Universidad Tecnica Federico Santa Maria, Valparaiso 1680, Chile
[4]Faculty of Engineering, Universidad San Sebastian, Santiago 8310639, Chile

CORRESPONDING AUTHOR: JORGE RODAS (e-mail: jrodas@ing.una.py)

This work was supported in part by Facultad de Ingeniería, Universidad Nacional de Asunción, Paraguay, in part by Consejo Nacional de Ciencia y Tecnología (CONACYT)–Paraguay under Project PINV01-272, in part by the "Programa de Incentivos para la Formación de Investigadores en Posgrados Nacionales under Grant BCAS02 for the "Programa de Doctorado en Ingeniería Electrónica, in part by the Government of Galicia under Grant GPC-ED431B 2023/12, in part by the Spanish State Research Agency (AEI) under Project PID2022-136908OBI00/MCIN/AEI/10.13039/501100011033/FEDER-UE, in part by ANID under Project AFB240002, in part by the Advanced Center for Electrical and Electronics Engineering FONDECYT under Grant 1230250, Grant FONDECYT 1241099, and Grant SERC (ANID/FONDAP/1522A0006), and in part by Thematic Network RIBIERSE-CYTED under Grant 723RT0150.

**ABSTRACT** Model predictive control has become a powerful and versatile control strategy, particularly effective in controlling multiphase machines. One of its key advantages is the ability to address multiple control objectives by incorporating constraints directly into the cost function. However, this feature typically necessitates the challenging task of tuning weighting factors to balance competing objectives effectively. This paper proposes a sequential model predictive torque control strategy for six-phase induction machines, eliminating the need for weighting factors. The proposed approach simplifies the control design process while maintaining high performance. Simulation and experimental results demonstrate the method's effectiveness, showing accurate torque, flux tracking, and appropriate stator currents regulation in the $\alpha - \beta$ and $x - y$ planes. These results highlight the potential of the proposed control strategy for practical implementation in advanced multiphase drive systems.

**INDEX TERMS** Multiphase electric machines, model predictive control (MPC), sequential model predictive control (SMPC), six-phase induction machine, torque control, weighting factor elimination.

## I. INTRODUCTION

Model Predictive Control (MPC) has emerged as a competitive control technique, gaining popularity in high-performance industrial applications, particularly in multiphase electric drives [1]. Its flexibility allows multiple control objectives to be incorporated within a single cost function while ensuring a rapid dynamic response. MPC has become a strong alternative to traditional strategies such as Direct Torque Control (DTC) and Field-Oriented Control (FOC) [2], as well as nonlinear approaches like Sliding-Mode Control (SMC), which, despite their robustness, can introduce undesirable chattering effects [3].

Multiphase electric machines offer advantages over traditional three-phase systems, including inherent fault tolerance [4], lower harmonic distortion [5], and improved power density [6]. Additionally, they enhance efficiency by reducing per-phase current, minimizing thermal stress, and enabling advanced control strategies [7]. These characteristics make them ideal for high-reliability applications such as electric vehicles, renewable energy systems, and marine propulsion [8].

However, controlling multiphase machines introduces challenges due to the increased number of phases, which requires advanced control strategies to manage independent subspaces such as the $\alpha - \beta$ and $x - y$ planes [9]. The complexity of multi-objective optimization makes traditional control methods like DTC, FOC and SMC less effective [10]. These challenges have driven the exploration of advanced control methods, with MPC emerging as a promising alternative that efficiently manages multiple control objectives while fully exploiting the capabilities of multiphase systems [11].

A key feature of MPC is its reliance on a cost function to optimize control objectives. This often requires weighting factors to balance competing goals such as torque, flux, switching losses, and current regulation. However, tuning these factors is challenging, as it depends on system-specific parameters and lacks a systematic design methodology. This issue is widely recognized, leading to research efforts exploring alternative solutions, including adaptive weighting strategies, multi-layer optimization, and methods that eliminate weighting factors altogether [12], [13].

Among these alternatives, Sequential Model Predictive Control (SMPC) has emerged as an effective strategy that addresses several limitations of conventional MPC. By prioritizing and addressing control objectives sequentially rather than within a single cost function [14], SMPC eliminates complex weighting factor tuning while maintaining high performance. Additionally, it reduces computational burden by decomposing the multi-objective problem into simpler hierarchical subproblems, making real-time implementation more feasible [15]. These benefits position SMPC as a practical approach for high-performance motor drive applications [16].

Several recent studies have investigated SMPC approaches for motor control applications. However, most research has been confined to three-phase systems, with little exploration of their applicability to multiphase machines. The first application of SMPC, presented in [19], demonstrated its effectiveness in three-phase machines by sequentially evaluating torque and flux control, eliminating the need for weighting factors. Davari et al. introduced a balanced SMPC method that dynamically prioritizes either torque or flux based on cross-error minimization, further enhancing performance [20]. Murillo-Yarce et al. compared various SMPC strategies across different converter topologies, highlighting the trade-offs between Voltage Source Inverter (VSI) and Neutral Point Clamped (NPC) converters regarding harmonic distortion and dynamic response [21]. Additionally, Shahid et al. reviewed MPC techniques for energy-efficient AC drives, emphasizing how sequential approaches reduce computational demands and improve steady-state performance [22]. In [23] was proposed a general strategy of SMPC that is effective when any of the two cost functions is first evaluated, so the hierarchy of the cost functions is solved, increasing the stability and universality of the SMPC.

In the context of multiphase machines, some Predictive Torque Control (PTC) strategies have been explored to address the added control complexity and subspace interactions. Gonçalves et al. [24] provided a comprehensive overview of predictive control methods for six-phase machines, emphasizing the challenges of weighting factor selection and converter configuration. Riveros et al. [25] introduced a PTC method for five-phase induction motor drives as a high-performance alternative to DTC. Their work offered improved response and reduced complexity. Luo and Liu [26] proposed a multi-vector-based MPTC strategy for six-phase permanent magnet synchronous machines (PMSMs), combining synthesized vectors and null vectors to maintain fixed switching frequency while effectively reducing current harmonics and torque ripple. Maqueda et al. [27] developed a reduced-complexity PTC algorithm for six-phase induction machines fed by a multi-modular matrix converter, demonstrating robust performance under speed control and fault conditions with significantly lower computational burden. These studies underline the relevance of MPTC in multiphase systems and motivate the development of sequential strategies like the one proposed in this paper.

This article builds upon the preliminary work presented in [28], where the fundamental concept of Sequential Model Predictive Torque Control (SMPTC) for six-phase induction machines was introduced. While the foundational principles were established, this study expands and refines the strategy by incorporating comprehensive experimental validation, a detailed analysis of implementation challenges, and optimizations to enhance robustness under varying operating conditions. This refined approach extends the applicability of SMPTC and establishes a new benchmark for high-performance predictive control in multiphase drive applications.

The main contributions of this article are summarized as follows:

1) The MPC is applied to a multiphase drive system, focusing on current and torque control. This offers a novel strategy that improves control performance and system efficiency.
2) The application of SMPC to a three-stage system exploits additional degrees of freedom, particularly in managing independent control subspaces and optimizing torque production efficiently. Currently, the literature applies SMPC only to a two-stage control structure, demonstrating its benefits in this type of application.
3) The proposed control strategy is tailored explicitly for six-phase induction machines. This expanded framework provides greater control flexibility, enabling superior management of the $\alpha - \beta$ and $x - y$ subspaces, which is crucial for adequate torque and flux regulation.

This paper is organized as follows: Section II details the modelling of the six-phase induction machine and associated predictive equations. Section III describes the proposed weighting-factorless SMPTC strategy. Section IV presents the simulation and experimental results, thoroughly analyzing the system's performance. Finally, Section V concludes the paper and outlines potential directions for future research.

## II. SIX-PHASE ELECTRIC MOTOR DRIVE'S MODEL

This study considers a six-phase induction machine with an asymmetric winding configuration and isolated neutrals. Two three-phase VSIs power the machine, each supplying an independent set of three-phase stator windings. The DC link voltage is denoted as $V_{dc}$. The system model is developed using the Vector Space Decomposition (VSD) method, which separates the control variables into the $\alpha - \beta$ and $x - y$ planes.

To account for inherent computational and actuation delays in the digital control system, a two-step prediction horizon $(k+2)$ is employed for delay compensation. This ensures that the control input applied at time $k$ anticipates system delays, thereby improving the precision and dynamic performance of the predictive control strategy. The discrete-time state-space representation of the system, incorporating this delay compensation mechanism, is formulated as:

$$\hat{\mathbf{i}}_{s[k+2|k]} = \mathbf{\Phi}\mathbf{i}_{s[k+1]} + \mathbf{\Gamma}\mathbf{v}_{s[k+1]} + \mathbf{\Gamma}_{\psi[k+1]}\boldsymbol{\psi}_{r[k+1]}, \tag{1}$$

where $\mathbf{i}_{s[k]} = \begin{bmatrix} i_{s\alpha[k]} & i_{s\beta[k]} & i_{sx[k]} & i_{sy[k]} \end{bmatrix}^T$ represents the stator currents, $\mathbf{v}_{s[k]} = \begin{bmatrix} v_{s\alpha[k]} & v_{s\beta[k]} & v_{sx[k]} & v_{sy[k]} \end{bmatrix}^T$ denotes the stator voltages, and $\boldsymbol{\psi}_{r[k]} = \begin{bmatrix} \psi_{r\alpha[k]} & \psi_{r\beta[k]} & 0 & 0 \end{bmatrix}^T$ corresponds to the rotor flux components.

The system matrices are:

$$\mathbf{\Phi} = \lambda_r \mathbf{I}_4, \quad \mathbf{\Gamma} = \frac{T_s}{\sigma L_s}\mathbf{I}_4,$$

$$\mathbf{\Gamma}_{\psi}[k] = \frac{k_r T_s}{\sigma L_s}\begin{bmatrix} \frac{1}{\tau_r} & \omega_{r[k]} & 0 & 0 \\ -\omega_{r[k]} & \frac{1}{\tau_r} & 0 & 0 \\ 0 & 0 & 0 & 0 \\ 0 & 0 & 0 & 0 \end{bmatrix}.$$

where $\lambda_r = 1 - \frac{T_s}{\tau_r}$ and $\mathbf{I}_4$ is the $4 \times 4$ identity matrix. The electrical parameters are defined as:

$$k_r = \frac{L_m}{L_r}, \quad \sigma = 1 - \frac{L_m^2}{L_s L_r}, \quad \tau_r = \frac{L_r}{R_r},$$

where $T_s$ is the sampling period, $\omega_{r[k]}$ is the rotor electrical speed, and $R_r, L_s, L_r, L_m$ are the machine parameters.

### A. VSI MODEL

The VSI model is characterized by $N = 2^6 = 64$ switching states, comprising 49 non-redundant and 15 redundant voltage vectors. The stator voltage vector $\mathbf{v}_{s[k]}$ is given by:

$$\mathbf{v}_{s[k]} = \frac{V_{dc}}{3}\mathbf{M}\mathbf{S}, \tag{2}$$

where the inverter transformation matrix $\mathbf{M}$ is:

$$\mathbf{M} = \begin{bmatrix} 2 & 0 & -1 & 0 & -1 & 0 \\ 0 & 2 & 0 & -1 & 0 & -1 \\ -1 & 0 & 2 & 0 & -1 & 0 \\ 0 & -1 & 0 & 2 & 0 & -1 \\ -1 & 0 & -1 & 0 & 2 & 0 \\ 0 & -1 & 0 & -1 & 0 & 2 \end{bmatrix}. \tag{3}$$

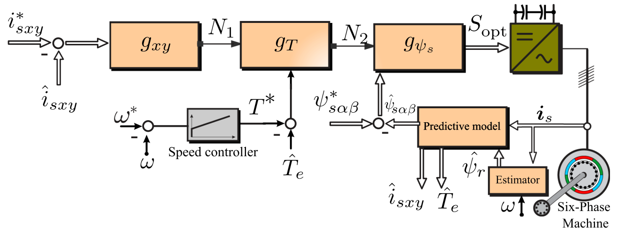


**FIGURE 1.** Proposed SMPTC strategy.

## III. PREDICTIVE TORQUE CONTROL

To implement the SMPTC strategy, predictive equations are used to estimate torque, flux, and stator currents at the prediction horizon $k+2$. The two-step prediction horizon is chosen to address delays caused by sampling, actuation, and computation, ensuring that the control action applied at time $k$ aligns with the actual system state when executed [29], [30]. The predicted electromagnetic torque is computed as:

$$\hat{T}_{e[k+2]} = 3P\left(\hat{\psi}_{s\alpha[k+2]}\hat{i}_{s\beta[k+2]} - \hat{\psi}_{s\beta[k+2]}\hat{i}_{s\alpha[k+2]}\right). \tag{4}$$

The predicted stator flux components are given by:

$$\hat{\boldsymbol{\psi}}_{s\alpha\beta[k+2]} = \sigma L_s \hat{\mathbf{i}}_{s\alpha\beta[k+2]} + k_r \boldsymbol{\psi}_{r\alpha\beta[k+2]}. \tag{5}$$

The rotor flux is estimated and predicted using the following expression, which serves as the internal flux estimator in the control scheme:

$$\hat{\boldsymbol{\psi}}_{r\alpha\beta[k+2]} = \lambda_r \boldsymbol{\psi}_{r\alpha\beta[k+1]} + \frac{L_m T_s}{\tau_r}\mathbf{i}_{s\alpha\beta[k+1]} - \omega_{r[k+1]}T_s \begin{bmatrix} 0 & 1 \\ -1 & 0 \end{bmatrix}\boldsymbol{\psi}_{r\alpha\beta[k+1]}. \tag{6}$$

### A. PROPOSED SMPTC

The proposed SMPTC strategy employs a three-stage sequential selection process, as illustrated in Fig. 1, which progressively refines voltage vector candidates. The control stages are:

*Stage 1:* $x$–$y$ Current Regulation: The first step minimizes $i_{sxy}$ by evaluating all $N = 64$ voltage vectors with the cost function:

$$g_{xy} = |i_{sxy}^* - \hat{i}_{sxy[k+2]}|. \tag{7}$$

This cost function is designed to minimize prediction errors in the $x$ and $y$ current components related to copper losses in multiphase machines. Since the reference is usually set to zero, this stage helps reduce these components. The formulation adheres to standard predictive control practices, where reference variables are tracked by minimizing their absolute deviation.

*Stage 2:* Torque Regulation: The best $N_1$ voltage vectors are selected for torque control using:

$$g_T = |T^* - \hat{T}_{e[k+2]}|. \tag{8}$$

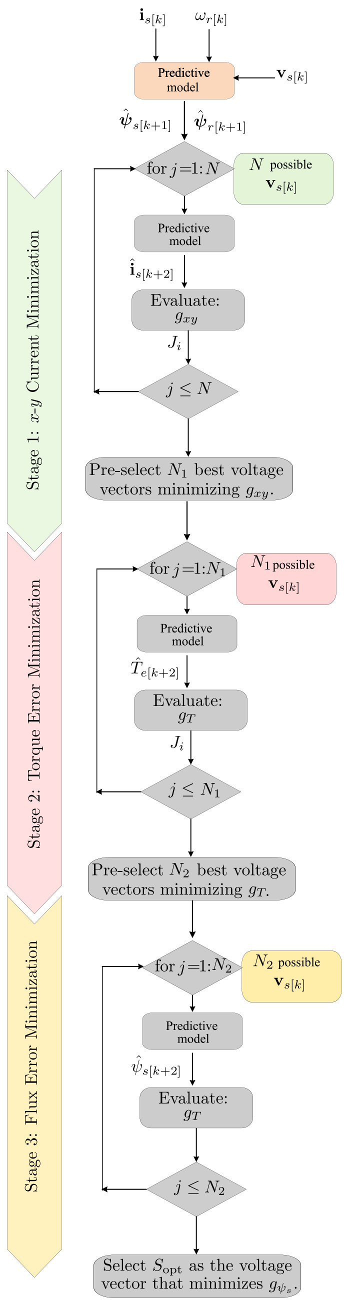


**FIGURE 2.** Flowchart of the proposed SMPTC implementation.

*Stage 3:* Flux Regulation: The best $N_2$ voltage vectors proceed to the final stage, minimizing:

$$g_{\psi_s} = |\psi^*_{s\alpha\beta} - \hat{\psi}_{s\alpha\beta[k+2]}|. \quad (9)$$

Finally, the optimal voltage vector minimizing $g_{\psi_s}$ is applied to the machine.

### B. FLOWCHART OF THE PROPOSED SMPTC STRATEGY

The entire SMPTC process is summarized in Fig. 2, which illustrates the step-by-step sequence followed by the predictive control strategy.

**TABLE 1.** Six-Phase Machine Electrical and Mechanical Parameters

| Parameter | Value | Parameter | Value |
|---|---|---|---|
| Rotor resistance | 6.9 ohms | Rotor inductance | 626.8 mH |
| Rated power | 2 kW | DC link voltage | 400 V |
| Stator resistance | 6.7 ohms | Nominal speed | 2540 rpm |
| Leakage inductance | 5.3 mH | Stator inductance | 654.4 mH |
| Moment of inertia | 0.07 kg·m$^2$ | Viscous friction coefficient | 0.0004 kg·m$^2$/s |
| Mutual inductance | 614 mH | Number of pole pairs | 1 |
| Rated AC voltage | 220 V | Rated frequency | 50 Hz |

The flowchart details the selection of voltage vectors across the three prediction stages, where each stage refines the candidate vectors based on the hierarchical cost functions. The flow begins with evaluating $N = 13$ switching states and selecting the best candidates for each subsequent control stage. This structure ensures reduced computational complexity while maintaining high-performance predictive control.

## IV. OBTAINED RESULTS

The proposed SMPTC strategy was validated using an experimental test bench featuring a six-phase induction machine powered by a dual three-phase VSI. The inverters are supplied by a controlled DC voltage source and managed through a dSPACE MABXII real-time control system. This system operates with MATLAB/Simulink for signal processing and implementation. Experimental data is recorded and processed using MATLAB. The electrical and mechanical parameters of the machine were identified using industry-standard standstill tests and AC time-domain analysis. The key machine parameters are listed in Table 1.

Hall effect sensors (LA 55-P), featuring a frequency response of up to 200 kHz, were used to measure the stator currents. The acquired signals are digitized with a 16-bit analog-to-digital (A/D) converter for precise processing. Rotor position feedback is obtained using a 1024-pulse-per-revolution (ppr) incremental encoder, from which speed estimation is derived. The machine is loaded with a 5 HP eddy current brake, allowing for the application of controlled torque.

The control strategy maintains the $x - y$ current references at zero ($i^*_{sx} = i^*_{sy} = 0$), as these components are primarily linked to additional power losses. Fig. 3 illustrates a schematic diagram of the experimental setup and includes images of the test bench.

### A. ANALYSIS OF $N_1$ AND $N_2$ SELECTION

The selection of $N_1$ and $N_2$ significantly impacts the performance of the proposed SMPTC strategy. These parameters determine the number of voltage vectors retained at each control stage, affecting the system response. Their effect is evaluated using the Total Harmonic Distortion (THD) of stator currents, the Mean Squared Error (MSE) of torque, and the MSE of $x - y$ current components.

Simulations were performed for different values of $N_1$ and $N_2$, and the corresponding THD, torque MSE, and $x - y$ current MSE are presented in Table 2.

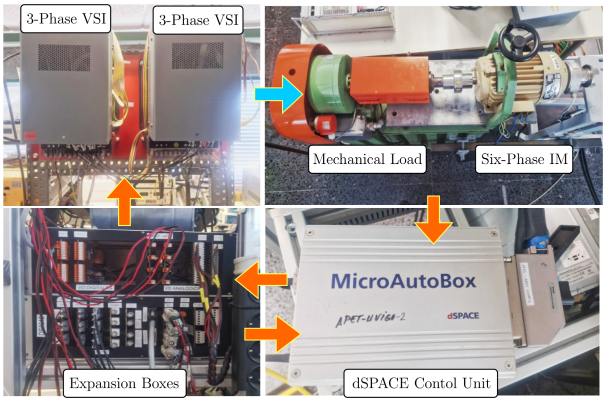


**FIGURE 3.** Experimental setup.

**TABLE 2.** Performance Evaluation of Different Combinations of $N_1$ and $N_2$ Based on THD, Torque MSE, and $x-Y$ Current MSE

| $N_1$ | $N_2$ | THD (%) | MSE ($T_e$) | MSE ($i_{sxy}$) |
|---|---|---|---|---|
| 11 | 2 | 11.844 | 0.029758 | 0.055494 |
| 11 | 3 | 11.499 | 0.028202 | 0.011966 |
| 11 | 4 | 11.172 | 0.026001 | 0.095337 |
| 11 | 5 | 11.435 | 0.050342 | 0.013776 |
| 12 | 2 | 11.978 | 0.028961 | 0.16677 |
| 12 | 3 | 11.288 | 0.027335 | 0.070524 |
| 12 | 4 | 11.226 | 0.026125 | 0.07521 |
| 12 | 5 | 14.116 | 0.076259 | 0.31988 |
| 13 | 2 | 12.151 | 0.027908 | 0.25262 |
| 13 | 3 | 10.766 | 0.02877 | 0.20143 |
| 13 | 4 | 10.863 | 0.025415 | 0.11998 |
| 13 | 5 | 11.817 | 0.020392 | 0.5445 |

According to Table 2, the values $N_1 = 13$ and $N_2 = 4$ represent a balanced trade-off among current distortion, torque tracking accuracy, and minimization of $x-y$ currents. This combination achieves an optimal compromise between current quality, torque regulation, and efficiency, making it suitable for real-time implementation.

### *B. EXPERIMENTAL VALIDATION*

In the first selection stage, $N = 13$ voltage vectors were considered. These vectors correspond to the outermost positions in the $\alpha-\beta$ plane, which yield smaller vector magnitudes when transformed into the $x-y$ plane. This selection naturally minimizes the influence of the $x-y$ components, primarily related to additional machine losses, thereby enhancing overall efficiency.

For clarity and reproducibility, Table 3 summarises all control-related parameters used in the implementation of the SMPTC strategy, including the prediction horizon, vector selection sizes, sampling time, and reference values.

Experimental tests were conducted under both steady-state and transient conditions, with a load set at 80% of the nominal torque. The purpose of these tests was to evaluate system performance across various operating conditions.

**TABLE 3.** Control Parameters Used in the Proposed SMPTC Algorithm

| Parameter | Value |
|---|---|
| Prediction horizon | 2 steps ($k+2$) |
| Sampling time $T_s$ | 50 $\mu s$ (20 kHz) |
| Evaluated voltage vectors $N$ | 13 |
| Selected vectors in Stage 1 ($N_1$) | 13 |
| Selected vectors in Stage 2 ($N_2$) | 4 |
| Reference $i^*_{sx}$, $i^*_{sy}$ | 0 A |
| Torque reference $T^*$ | Application-dependent |
| Flux reference $\psi^*_{s\alpha\beta}$ | Based on nominal parameters |

#### 1) COMPARISON BETWEEN CONVENTIONAL PTC AND THE PROPOSED SMPTC

The conventional PTC strategy used for comparison is based on standard predictive control formulations, as described in [24], and includes torque, flux, and *x*–*y* current regulation through a weighted cost function. To enable a fair performance comparison with the proposed SMPTC, the weighting factors in the classic PTC scheme were heuristically tuned. Several combinations of $K_f$ (flux weighting) and $K_x$, $K_y$ (for *x*–*y* current terms) were tested to achieve acceptable system behavior across different operating conditions. It was observed that high values of $K_f$, $K_x$, and $K_y$ excessively penalize the associated variables, degrading torque response. Conversely, very low weights allow excessive *x*–*y* currents, increasing losses. The best trade-off was achieved with $K_f = 10$, and $K_x = K_y = 0.2$, resulting in reduced torque ripple and controlled *x*–*y* current components. Further implementation details are available in Appendix A. For consistency, the same sampling frequency was used in both control strategies to ensure a fair and technically sound comparison.

In the classical implementation of PTC, all 64 voltage vectors are evaluated at each sampling instant, thanks to the computational structure that allows for full enumeration. In contrast, the SMPTC algorithm uses sequential selection and limits the number of evaluated vectors to 13 to ensure real-time applicability. The selected vectors are those deemed to have the highest potential impact based on control goals.

Fig. 4 presents a steady-state analysis of the motor operating at 1500 r/min, comparing classic PTC (left column) and SMPTC (right column). The top graphs in both columns display the torque response, demonstrating rapid stabilization under steady-state conditions. The second and third graphs show the stator flux and speed, respectively, for both control techniques. The stator currents in the $\alpha-\beta$ plane are represented in fourth graphs, where SMPTC shows a lower ripple than classic PTC. The fifth set of graphs represents the stator currents in the $x-y$ plane, indicating that SMPTC reduces losses compared to classic PTC. This comparison emphasizes the advantages of SMPTC in steady-state operation.

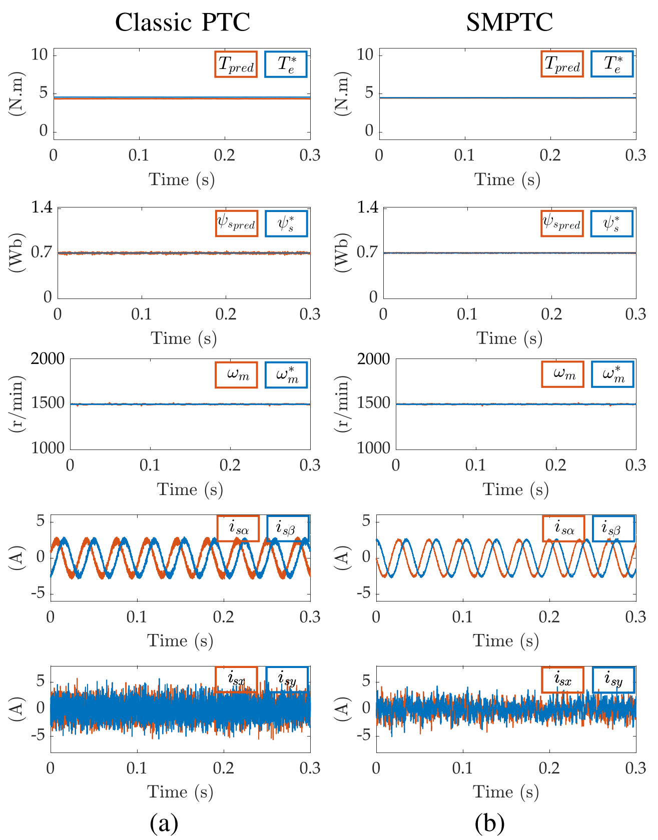


**FIGURE 4.** Steady-state analysis at 80% of nominal torque running at 1500 r/min: From top to bottom for both classic PTC (left column) and SMPTC (right column): Torque; flux; speed; $\alpha-\beta$ stator currents and $x-y$ stator currents.

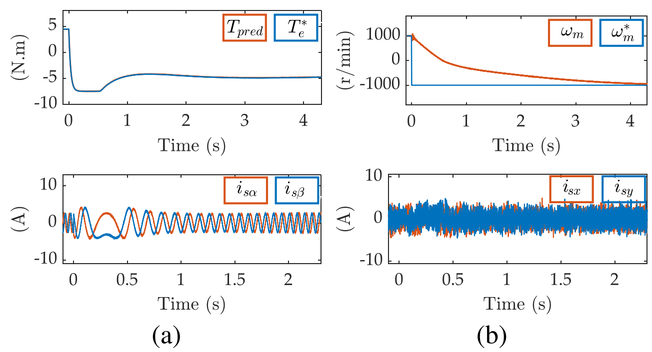


**FIGURE 5.** Reverse test from 1000 r/min to −1000 r/min: From top to bottom (left column): Torque and $\alpha-\beta$ stator currents; (right column): Rotor mechanical speed and $x-y$ stator currents.

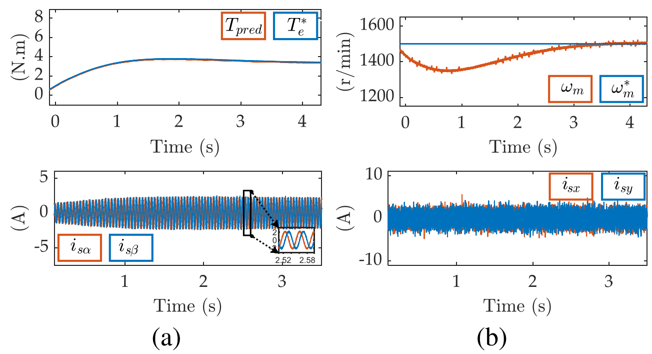


**FIGURE 6.** Torque response at 80% of nominal torque at 1500 r/min: From top to bottom (left column): Torque and $\alpha-\beta$ stator currents; (right column): Rotor mechanical speed and $x-y$ stator currents.

**TABLE 4.** Computational Cost and Switching Frequency Comparison

| Metric | Classic PTC | Proposed SMPTC |
|---|---|---|
| Structure | Single-stage | Three-stage |
| Floating point operations (FPOs) | 3968 | 1958 |
| Avg. switching frequency | 3.6 kHz | 5.8 kHz |

To complement the performance comparison, Table 4 summarizes the computational effort and switching frequency for both control strategies. A detailed analysis shows that, for each iteration, the SMPTC algorithm performs 123 Floating-Point Operations (FPOs) related to flux and current prediction, and 117 additional FPOs due to the two-step prediction horizon. The cost function minimization involves three loops: the first loop for $x$–$y$ current regulation with 13 iterations performs 845 FPOs, the second loop for torque control with 13 outer and 4 inner iterations performs another 845 FPOs, and the third loop for flux control with 4 iterations adds 28 FPOs. This results in a total of 1958 FPOs per sampling period for the SMPTC strategy. On the other hand, for the classical PTC implementation, which evaluates all 64 voltage vectors at once across a single-stage cost function, the total number of FPOs per sampling period is 3968.

In addition to the computational effort, Table 4 also compares the average switching frequency of both control strategies. The results show that the proposed SMPTC exhibits a higher average switching frequency (5.8 kHz) compared to the classic PTC (3.6 kHz).

### 2) DYNAMIC ANALYSIS OF THE SMPTC

Next, Fig. 5 presents the results of the reverse test, where the motor speed transitions from 1000 r/min to -1000 r/min. The left column illustrates the torque response and the stator currents in the $\alpha-\beta$ plane. It shows a rapid decrease in torque followed by stabilization as the motor changes direction. During this transition, the stator currents exhibit significant oscillations. The right column displays the rotor's mechanical speed, which shifts from positive to negative, confirming the successful reversal of motor operation. The second graph on the right depicts the stator currents in the $x-y$ plane, which stabilize after an initial transient period. This figure effectively demonstrates the motor's dynamic response during the reversal process.

Fig. 6 illustrates the transient response of the torque when operating at 80% of the nominal load, with the motor running at a constant speed of 1500 r/min. The top graph shows that the torque quickly stabilizes at its reference value after a brief

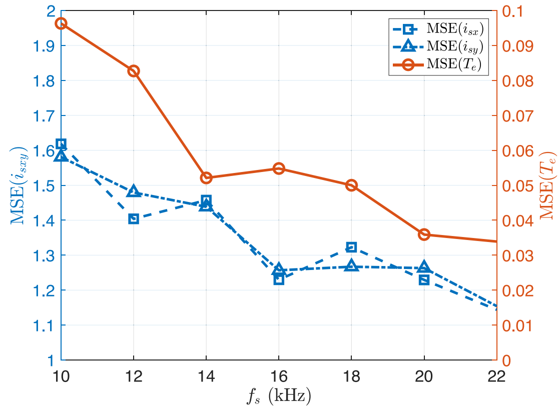


**FIGURE 7. Effect of Sampling Frequency on Torque and Current Errors.**

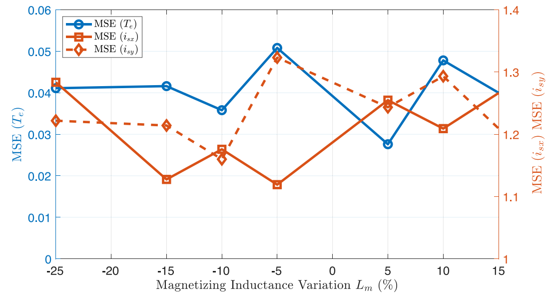


**FIGURE 8. Performance Sensitivity to Magnetizing Inductance Variation.**

transient period. During this transition, the rotor speed experiences a slight drop before returning to its steady-state value. The figure is organized into two columns. The left column presents the torque response and the stator currents in the $\alpha - \beta$ plane, oscillating around their steady-state values. The right column displays the rotor's mechanical speed, which stabilizes rapidly, along with the stator currents in the $x - y$ plane, which settle after an initial transient period. This figure emphasizes the motor's torque response and smooth transition to the desired operating conditions.

### 3) SENSITIVITY ANALYSIS TO SAMPLING FREQUENCY AND PARAMETER VARIATIONS

Fig. 7 illustrates how the sampling frequency ($f_s$) affects the MSE of $T_e$ and the stator current components in the $x - y$ plane ($i_s$). The graph shows that as the sampling frequency increases, the MSE values generally decrease, indicating improved control accuracy. Specifically, the MSE of Te drops significantly from 0.0963 at 10 kHz to approximately 0.0339 at 22 kHz, highlighting that higher sampling rates enhance torque regulation. Similarly, the MSE also follows a decreasing trend, reflecting a reduction in unwanted current components that contribute to power losses. However, beyond 16 kHz, the improvement in MSE becomes less pronounced, suggesting a potential trade-off between performance gains and computational burden. This analysis emphasizes the importance of selecting an optimal sampling frequency to balance control precision and implementation feasibility in predictive torque control strategies.

Finally, the impact of magnetizing inductance ($L_m$) variations on control performance is analyzed in Fig. 8. The horizontal axis represents deviations of $L_m$ from its nominal value, where 1.0 corresponds to the baseline. In contrast, the left vertical axis shows the MSE of $i_{sx}$ and $i_{sy}$, and the right vertical axis represents the MSE of $T_e$. The results indicate that while parameter variations influence the control performance, the proposed SMPTC strategy maintains a stable response, demonstrating robustness against model uncertainties. The fluctuations in MSE values remain within acceptable limits, confirming the method's effectiveness under varying system parameters.

Note that the proposed control strategy utilizes a single voltage vector for each sampling period. While this approach simplifies the algorithm and allows for real-time implementation, it may result in slightly higher torque ripple compared to methods that use multiple vectors per cycle. However, these multi-vector strategies often bring about increased modulation complexity and additional computational demands.

## V. CONCLUSION

This paper introduced a novel Sequential Model Predictive Torque Control (SMPTC) strategy for six-phase induction machines, eliminating the need for weighting factors while effectively managing multiple control objectives. By implementing a three-stage sequential selection process, the proposed method prioritized $x$-$y$ current regulation, torque tracking, and flux control separately, improving system performance regarding current quality, torque accuracy, and computational efficiency. The selection of $N_1 = 13$ and $N_2 = 4$ provided an optimal balance between minimizing harmonic distortion and maintaining accurate torque regulation, as demonstrated through simulation and experimental validation. The results confirmed that SMPTC outperforms conventional predictive control strategies by reducing the ripple of the stator current and improving steady-state and transient performance.

Although several recent works have addressed the reduction of computational complexity and the tuning of weighting factors in MPC for multiphase machines—through auto-tuning methods, metaheuristic optimization, or simplified cost functions—these approaches still depend on the presence of weighting parameters and often require extensive offline adjustment. In contrast, the main contribution of the proposed SMPTC strategy lies in fully eliminating the need for weighting factors by sequentially prioritizing control objectives, which simplifies implementation and enhances robustness without relying on heuristic tuning.

Future work will further optimise the selection of $N_1$ and $N_2$ through a systematic methodology, reducing computational complexity via advanced selection algorithms and enhancing robustness against parameter variations. Extending the proposed strategy to other multiphase machine configurations and integrating fault-tolerant capabilities could broaden its applicability in industrial and automotive drive systems.

## APPENDIX CONVENTIONAL PREDICTIVE TORQUE CONTROL (PTC) METHOD

In this approach, the outer loop comprises a conventional PI controller that regulates the mechanical speed and generates the corresponding torque reference $T_e^*$, similarly to the proposed SMPTC. This reference is compared against the predicted electromagnetic torque, which is calculated using the predictive model and depends on both estimated and forecasted rotor flux components.

In addition, the stator flux is predicted and compared to its reference value. The algorithm evaluates all available switching states defined by the converter (a total of 64 vectors in this case), using real-time measurements of rotor speed and stator phase currents as inputs to the model.

A key feature of this method is the use of a cost function, shown in (10), which combines multiple control objectives—namely torque, flux, and $x$–$y$ current regulation. This is achieved through a set of weighting factors, $K_f$, $K_x$, and $K_y$, which balance the influence of each term in the minimization process and must be tuned according to specific application needs. These factors directly influence the selection of the optimal switching vector to be applied during each sampling interval.

$$J = (e_{torque})^2 + K_f(e_{flux})^2 + K_x(e_x)^2 + K_y(e_y)^2 \tag{10}$$

where the errors are defined as: $e_{torque} = T_e^* - T_{e[k+2]}$, $e_{flux} = \psi_s^* - \psi_{s[k+2]}$, $e_x = i_{sx}^* - i_{sx}$, $e_y = i_{sy}^* - i_{sy}$.

## REFERENCES


[1] J. Rodriguez et al., "Latest advances of model predictive control in electrical drives—Part II: Applications and benchmarking with classical control methods," *IEEE Trans. Power Electron.*, vol. 37, no. 5, pp. 5047–5061, May 2022, doi: 10.1109/TPEL.2021.3121589.

[2] J. Rodriguez et al., "Latest advances of model predictive control in electrical drives—Part I: Basic concepts and advanced strategies," *IEEE Trans. Power Electron.*, vol. 37, no. 4, pp. 3927–3942, Apr. 2022, doi: 10.1109/TPEL.2021.3121532.

[3] J. Rodas, I. Gonzalez-Prieto, Y. Kali, M. Saad, and J. Doval-Gandoy, "Recent advances in model predictive and sliding mode current control techniques of multiphase induction machines," *Front. Energy Res.*, vol. 9, no. 15, Art. no. 729034, 2021.

[4] Z. Wang, X. Wang, Y. Wang, J. Chen, and M. Cheng, "Fault tolerant control of multiphase multilevel motor drives - Technical review," *Chin. J. Elect. Eng.*, vol. 3, no. 2, pp. 76–86, Sep. 2017.

[5] K. Nounou, J. F. Charpentier, K. Marouani, M. Benbouzid, and A. Kheloui, "Emulation of an electric naval propulsion system based on a multiphase machine under healthy and faulty operating conditions," *IEEE Trans. Veh. Technol.*, vol. 67, no. 8, pp. 6895–6905, Aug. 2018.

[6] M. Gholamian, O. Beik, and M. Arshad, "A review of state-of-the-art multiphase and hybrid electric machine," *Electronics*, vol. 13, no. 18, 2024, Art. no. 3636.

[7] K. Ni et al., "Electrical and electronic technologies in more-electric aircraft: A review," *IEEE Access*, vol. 7, pp. 76145–76166, 2019.

[8] M. Zhang, M. Yuan, and J. Jiang, "A comprehensive review of the multiphase motor drive topologies for high-power electric vehicle: Current status, research challenges, and future trends," *IEEE Trans. Transport. Electrific.*, vol. 11, no. 1, pp. 3631–3654, Feb. 2025.

[9] M. Bermudez, C. Martín, I. Gonzalez-Prieto, M. J. Duran, M. R. Arahal, and F. Barrero, "Predictive current control in electrical drives: An illustrated review with case examples using a five-phase induction motor drive with distributed windings," *IET Electric Power Appl.*, vol. 14, pp. 1291–1310, 2020.

[10] Z. Zhang, J. Zhang, Y. Wu, Z. Zhu, and S. Chang, "A weighted-free CCS model predictive current control with implicit modulation for DTP-PMSMs," *IEEE Trans. Ind. Electron.*, vol. 72, no. 4, pp. 3335–3345, Apr. 2025.

[11] Z. Yu and J. Long, "Review on advanced model predictive control technologies for high-power converters and industrial drives," *Electronics*, vol. 13, no. 24, 2024, Art. no. 4969.

[12] S. Xu, C. Yao, G. Ren, Z. Sun, S. Wu, and G. Ma, "Weighting factors autotuning of FCS-MPC for hybrid ANPC inverter in PMSM drives based on deep residual networks," *IEEE Trans. Power Electron.*, vol. 39, no. 12, pp. 16540–16552, Dec. 2024.

[13] M. Monadi, M. Nabipour, F. Akbari-Behbahani, and E. Pouresmaeil, "Speed control techniques for permanent magnet synchronous motors in electric vehicle applications toward sustainable energy mobility: A review," *IEEE Access*, vol. 12, pp. 119615–119632, 2024.

[14] D. Prajapati, A. Dekka, D. Ronanki, and J. Rodriguez, "High-performance sequential model predictive control of a four-level inverter for electric transportation applications," *IEEE Trans. Emerg. Sel. Topics Power Electron.*, vol. 5, no. 1, pp. 253–262, Jan. 2024.

[15] T. Liu, X. Yao, J. Wang, and C. Ma, "Efficient two-vector-based sequential model predictive control for IM drives," *IEEE Trans. Emerg. Sel. Topics Power Electron.*, vol. 12, no. 1, pp. 903–912, Feb. 2024.

[16] K. Zhang et al., "Tolerant sequential model predictive direct torque control of permanent magnet synchronous machine drives," *IEEE Trans. Transport. Electrific.*, vol. 6, no. 3, pp. 1167–1176, Sep. 2020.

[17] M. R. Arahal, F. Barrero, M. G. Satue, and F. Colodro, "Voronoi multi-phase predictive current control with variable application times," *IEEE Trans. Energy Convers.*, early access, Nov. 15, 2024, doi: 10.1109/TEC.2024.3497212.

[18] A. Shawier, W. E. Abdel-Azim, M. G. Abdel-Moneim, S. Gadoue, A. S. Abdel-Khalik, and S. Ahmed, "Optimized virtual vector technique with loss minimization of six phase IM under low-speed operation for electric vehicles," *IEEE Trans. Transp. Electrific.*, vol. 11, no. 2, pp. 5748–5758, Apr. 2025.

[19] M. Norambuena, J. Rodriguez, Z. Zhang, F. Wang, C. Garcia, and R. Kennel, "A very simple strategy for high-quality performance of AC machines using model predictive control," *IEEE Trans. Power Electron.*, vol. 34, no. 1, pp. 794–800, Jan. 2019, doi: 10.1109/TPEL.2018.2812833.

[20] S. A. Davari, M. Norambuena, V. Nekoukar, C. Garcia, and J. Rodriguez, "Even-handed sequential predictive torque and flux control: A weighting factor-free model predictive strategy for high-performance motor drive applications," *IEEE Trans. Power Electron.*, vol. 35, no. 9, pp. 9053–9063, Sep. 2020.

[21] D. Murillo-Yarce, B. Araya, C. Restrepo, M. Rivera, and P. Wheeler, "Impact of sequential model predictive control on induction motor performance: Comparison of converter topologies," *Mathematics*, vol. 11, no. 4, Feb. 2023, Art. no. 972.

[22] M. B. Shahid et al., "Model predictive control for energy efficient AC motor drives: An overview," *IET Electric Power Appl.*, vol. 18, no. 10, pp. 1894–1920, Oct. 2024.

[23] Y. Zhang, B. Zhang, H. Yang, M. Norambuena, and J. Rodriguez, "Generalized sequential model predictive control of induction motor drives," in *Proc. 21st Int. Conf. Elect. Mach. Syst.*, Jeju, South Korea, 2018, pp. 1285–1290, doi: 10.23919/ICEMS.2018.8549339.

[24] P. Gonçalves, S. Cruz, and A. Mendes, "Finite control set model predictive control of six-phase asymmetrical machines—An overview," *Energies*, vol. 12, no. 24, 2019, Art. no. 4693.

[25] J. A. Riveros, F. Barrero, E. Levi, M. J. Durán, S. Toral, and M. Jones, "Variable-speed five-phase induction motor drive based on predictive torque control," *IEEE Trans. Ind. Electron.*,, vol. 60, no. 8, pp. 2957–2968, Aug. 2013.

[26] Y. Luo and C. Liu, "Multi-vector-Based model predictive torque control for a six-phase PMSM motor with fixed switching frequency," *IEEE Trans. Energy Convers.*, vol. 34, no. 3, pp. 1369–1379, Sep. 2019.

[27] E. Maqueda et al., "Speed control of a six-phase IM fed by a multi-modular matrix converter using an inner PTC with reduced computational burden," *IEEE Access*, vol. 9, pp. 160035–160047, 2021.

[28] J. Rodas et al., "Weighting-factorless sequential model predictive torque control of a six-phase AC machine," in *Proc. IEEE Conf. power Electron. Renewable Energy*, Luxor, Egypt, 2023, pp. 1–5, doi: 10.1109/CPERE56564.2023.10119622.

[29] P. Cortes, J. Rodriguez, C. Silva, and A. Flores, “Delay compensation in model predictive current control of a three-phase inverter,” *IEEE Trans. Ind. Electron.*, vol. 59, no. 2, pp. 1323–1325, Feb. 2012.

[30] J. Rodas, F. Barrero, M. R. Arahal, C. Martín, and R. Gregor, “On-line estimation of rotor variables in predictive current controllers: A case study using five-phase induction machines,” *IEEE Trans. Ind. Electron.*, vol. 63, no. 9, pp. 5348–5356, Sep. 2016.

**JORGE RODAS** (Senior Member, IEEE) received the Ph.D. degree from a Joint University Program between Universidad Nacional de Asuncion (UNA), San Lorenzo, Paraguay, and Universidad de Sevilla, Seville, Spain, in 2016. He is currently a Professor and the Research Director at the Facultad de Ingenieria, UNA. With more than 140 published papers, his research interests include advanced control applications for power electronic converters, renewable energy systems, and electric motor drives. Dr. Rodas was the recipient of the Paraguayan National Science Award. He served as Guest Editor of the IEEE Journal of Emerging and Selected Topics in Power Electronics and Associate Editor of IEEE Access. He is also a Fellow of the Institute of Engineering and Technology, U.K.

**OSVALDO GONZALEZ** was born in Asunción, Paraguay. He received the B.Eng. degree in electronic engineering from the Universidad Nacional de Asunción (UNA), San Lorenzo, Paraguay, in 2014, and the M.Sc. and Ph.D. degrees in power electronics from Engineering Faculty, UNA, in 2017 and 2021, respectively. His research focuses on the area of control of multiphase motors.

**PAOLA MAIDANA** received the degree in electronic engineering and the Master of Science degree in power electronics from the Facultad de Ingeniería de la Universidad Nacional de Asunción, San Lorenzo, Paraguay, where she is currently working toward the Doctoral degree in electronic engineering with Power and Control Systems Laboratory. Her research interests include nonlinear control of electrical drives, multiphase induction machines, and power electronic converters.

**CHRISTIAN MEDINA** received the degree in electronic engineering and the Master of Science degree in electronic engineering from the Facultad de Ingeniería de la Universidad Nacional de Asunción, San Lorenzo, Paraguay, where he is currently working toward the Doctoral degree. His research interests include electronic power converters, nonlinear control, and induction machines.

**JESÚS DOVAL-GANDOY** (Member, IEEE) received the M.S. degree in electrical engineering from the Polytechnic University of Madrid, Madrid, Spain, in 1991, and the Ph.D. degree in electrical engineering from the University of Vigo, Vigo, Spain in 1999. He is currently a Professor and the Head with the Applied Power Electronics Technology Research Group, University of Vigo. His research focuses on AC power conversion.

**MARGARITA NORAMBUENA** (Senior Member, IEEE) received the B.S. and M.Sc. degrees in electrical engineering, in 2013, the Ph.D. degree *(summa cum laude)* in electronics engineering from the Universidad Tecnica Federico Santa Maria, Valparaiso, Chile, in 2017, and the Doktoringenieur (Dr.-Ing.) degree *(summa cum laude)* in electrical and electronic engineering from the Technische Universitat Berlin (TUB), Berlin, Germany, in 2018. She is currently an Assistant Professor with Universidad Tecnica Federico Santa Maria. Her research interests include multilevel converters, model predictive control of power converters and drives, energy storage systems, renewable energy, and electromobility. She is also Associate Editor for IEEE JOURNAL OF EMERGING AND SELECTED TOPICS IN POWER ELECTRONICS. Dr. Norambuena was the recipient of the IEEE IES Student Best Paper Award 2019 for her doctoral work.

**MAGNO AYALA** (Member, IEEE) received the B.Eng. degree in electronic engineering from the Universidad Nacional de Asunción (UNA), San Lorenzo, Paraguay, in 2014, the M.Sc. and Ph.D. degrees in power electronics from the Faculty of Engineering, UNA, in 2017 and 2020, respectively. His research focuses on the areas of control of multiphase AC machines. He was the recipient of the Paraguayan National Science Award in 2020 and an Award from the Industrial Electronics Society in 2021.

**JOSE RODRIGUEZ** (Life Fellow, IEEE) received the Engineer degree in electrical engineering from the Universidad Tecnica Federico Santa Maria, Valparaiso, Chile, in 1977, and the Dr.-Ing. degree in electrical engineering from the University of Erlangen, Erlangen, Germany, in 1985. Since 1977, he has been with the Department of Electronics Engineering, Universidad Tecnica Federico Santa Maria, where he was a full Professor and the President. From 2015 to 2019, he was the President of Universidad Andres Bello, Santiago, Chile. From 2022 to 2023, he was the President with Universidad San Sebastian, Santiago. He is currently the Director with the Center for Energy Transition, Universidad San Sebastian. He has coauthored two books, several book chapters, and more than 900 journal and conference papers. His research interests mainly include multilevel inverters, new converter topologies, control of power converters, and adjustable-speed drives. Dr. Rodriguez was the recipient of the number of Best Paper awards from journals of the IEEE, National Award of Applied Sciences and Technology in 2014 from the Government of Chile, and Eugene Mittelmann Award in 2015 from the Industrial Electronics Society of the IEEE. From 2014 to 2024, he has been included in the list of Highly Cited Researchers published by Web of Science. Electronics Society. He is a Member of the Chilean Academy of Engineering.